Grain Structure in Block Copolymer Thin Films Studied by Guided Wave Depolarized Light Scattering

Bruce A. Garetz,*,† Maurice C. Newstein,‡ Jeffrey D. Wilbur,§ Amish J. Patel,§ David A. Durkee,§ Rachel A. Segalman,§,⊥ J. Alexander Liddle,⊥ and Nitash P. Balsara*,§,⊥,#

Othmer Department of Chemical and Biological Sciences and Engineering, Polytechnic University, Six Metrotech Center, Brooklyn, New York 11201; Department of Electrical Engineering, Polytechnic University, Six Metrotech Center, Brooklyn, New York 11201; Department of Chemical Engineering, University of California, Berkeley, Berkeley, California 94720; and Materials Sciences Division and Environmental Energy Technologies Division, Lawrence Berkeley National Laboratory, University of California, Berkeley, California 94720

Received October 15, 2004; Revised Manuscript Received February 3, 2005

ABSTRACT: A new optical technique for characterizing the grain structure of ordered block copolymer thin films has been developed. The technique, which we refer to as guided wave depolarized light scattering (GWDLS), is an adaptation of previous work wherein polarized light was used to characterize the grain structure in bulk block copolymer samples [Newstein et al. *Macromolecules* **1998**, *31*, 64]. Spin-casting and vacuum-annealing were used to prepare thin films of an ordered poly(α-methylstyrene-*block*-isoprene) copolymer on a flat, fused silica substrate. The ordered phase consisted of poly(α-methylstyrene) cylinders in a polyisoprene matrix. A plane-polarized laser beam was coupled into and out of a transverse magnetic (TM) mode of the film, which acts as a planar waveguide. The angle of incidence is adjusted to optimize the coupling efficiency into a particular mode of the waveguide. The path length traveled by the guided wave between the input and output coupling points was approximately 1 cm. The polarization of some of the incident light changes due to encounters with randomly oriented, optically anisotropic grains. This results in the coupling of light into propagating transverse electric (TE) modes in the sample. We show that the TE beam intensity of annealed samples with well-developed grain structure is significantly larger than that obtained from unannealed samples with poorly developed grain structure. The GWDLS results are consistent with atomic force microscopy results obtained from the annealed and unannealed films.

Introduction

Thin films composed of dense periodic structures on the nanometer length scale are expected to enable a wide variety of applications ranging from ultrahigh-density information storage to DNA electrophoresis.[1−5] Block copolymer thin films have been the subject of intense study due to their potential use in these applications. A variety of techniques such as neutron and X-ray reflectivity (NR and XR, respectively),[6−8] secondary ion mass spectrometry (SIMS),[9,10] atomic force microscopy (AFM),[11,12] scanning and transmission electron microscopy (SEM and TEM, respectively),[13,14] and grazing incidence small-angle X-ray scattering (GISAXS)[15−17] have been used to study these systems. The main purpose of this paper is to describe the development of guided wave depolarized light scattering (GWDLS), a new technique for probing the structure of ordered block copolymer thin films.

Characterizing systems in both reciprocal and position space is important due to the complementary nature of these techniques. Specular NR and XR are reciprocal space techniques that are sensitive to the presence of periodic order in the direction normal to the plane of the film. Complementary position space data can be obtained by SIMS and cross-sectional TEM. The lateral structure of block copolymer thin films has been studied in position space by TEM (of films on SiN windows), SEM, and AFM. The efforts of Harrison et al. and Segalman et al. to quantify defect density and defect annihilation in block copolymer thin films are particularly noteworthy.[3,18] GISAXS is the only reciprocal space technique able to study lateral structure in block copolymer thin films, but it provides no information on grain structure and requires a high-energy X-ray source. The GWDLS technique that we have proposed has the potential of filling this void, allowing lateral grain structure characterization in reciprocal space. Because of its nondestructive nature and relatively rapid data acquisition time, it is ideally suited for time-resolved measurements.

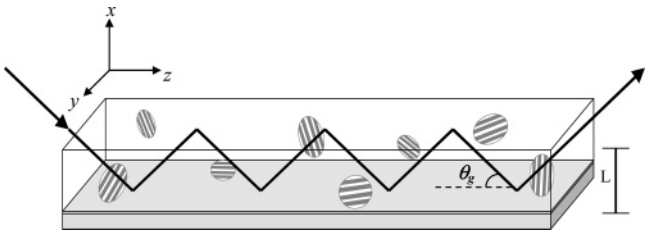

Figure 1. Schematic of light propagating through a partially ordered block copolymer film via total internal reflection in GWDLS.

The operating principle of GWDLS is depicted in Figure 1. A block copolymer thin film deposited on a fused silica substrate with a low index of refraction serves as a planar waveguide. A plane-polarized laser

† Othmer Department of Chemical and Biological Sciences and Engineering, Polytechnic University.
‡ Department of Electrical Engineering, Polytechnic University.
§ Department of Chemical Engineering, UC Berkeley.
⊥ Materials Sciences Division, Lawrence Berkeley National Laboratory.
Environmental Energy Technologies Division, Lawrence Berkeley National Laboratory.

10.1021/ma047859b CCC: $30.25
Published on Web 04/14/2005

beam is coupled into a transverse magnetic (TM) mode of the waveguide and thus travels through the length of the sample by total internal reflection. The light beam will propagate without scattering if the optic axes of the grains are either parallel or perpendicular to the plane of the film. However, grains with optic axes that are oblique relative to the plane of the film (misaligned grains) cause depolarized light scattering into the transverse electric (TE) modes of the waveguide. Both TE and TM modes are then coupled out of the film, and the TE component is isolated with the help of a crossed polarizer. The TE component is further isolated by a vertical slit that is positioned to allow the TE component to pass while blocking the TM component, which has a small angular offset. In principle, this technique should be applicable to any block copolymer that forms optically anisotropic ordered phases. Note that the optical anisotropy arises due to both form and intrinsic birefringence.[19]

GWDLS is an adaptation of previous work[20−27] wherein polarized light was used to study the grain structure of bulk block copolymer samples. The relationship between grain structure and the propagation and scattering of polarized light was studied in a series of papers. Individual, ordered grains of anisotropic block copolymer phases such as lamellae and cylinders arranged on a hexagonal lattice are optically equivalent to uniaxial crystals. Our early work was restricted to quiescently ordered systems composed of randomly oriented grains. In that case, we demonstrated that the fraction of incident power transmitted through a sample held between crossed polarizers is proportional to the average grain size.[21] In subsequent studies, we demonstrated that more quantitative information about the grain structure could be obtained by studying the angular spread of the exiting beam, i.e., from depolarized light scattering (DPLS) measurements.[22,23] Light scattering patterns with 4-fold symmetry indicate the presence of correlation between grain shapes and optic axes, while the presence of off-axis scattering peaks indicate that the optic axes and orientation of neighboring grains are correlated.[25] We also demonstrated that the evolution of grain structure could be determined from time-resolved DPLS measurements.[26,27] It is, perhaps, worth noting that the optical characterization of quiescently ordered, bulk block copolymers in now routinely done in other laboratories.[28−32] Lodge et al. have used DPLS to study order−order transitions between a birefringent cylindrical phase and a nonbirefringent gyroid phase.[28] More recently, Epps and co-workers have used DPLS to study phase transitions between two interconnected network phases, a cubic network phase and a noncubic network phase.[29] Migler and Han have used this technique to study block copolymer melts at elevated pressures.[30] In a similar vein, Watkins et al. have developed an apparatus to study the optical properties of mixtures of block copolymers and supercritical fluids at elevated pressures.[31] DPLS has also been used to study the grain structure of macroscopically aligned samples. Burghardt et al. demonstrated that DPLS could be used to characterize the grain structure of liquid crystalline polymers under flow.[32] Our group has shown that the combination of birefringence and DPLS measurements enables characterization of both the aligned single crystal and the coexisting unaligned grains.[25] The work presented in this paper is the first step toward enabling these kinds of measurements in thin films.

Experimental Methods

The experiments reported here were conducted on an anionically synthesized poly(α-methylstyrene-*block*-isoprene) copolymer (MSI). Standard high-vacuum procedures were used to conduct the reaction. Approximately 12 mL of hexane was distilled into a clean reactor on a high-vacuum line, and then 6 mL of purified α-methylstyrene monomer was distilled into the reactor using a short path connection. This was followed by the addition of 0.5 mL of 1.4 M *sec*-butyllithium (initiator) in an argon glovebox. The color of the mixture changes from clear to bright red. The reactor was then returned to the vacuum line and thoroughly degassed, and 250 mL of tetrahydrofuran (THF) was distilled into the reactor, using liquid nitrogen. Polymerization was allowed to proceed at −78 °C for 10 h. An aliquot of the living polymer was removed and terminated by isopropyl alcohol (IPA) for characterization purposes. 20 mL of isoprene was then distilled into the reactor, and the reaction was allowed to proceed for 4 h at −78 °C. The color of the reaction mixture changes from red to yellow during this step. To ensure completion of the reaction, the reaction was allowed to proceed at 0 °C for ca. 10 h and terminated using IPA. The total molecular weight of the MSI polymer was determined to be 32 kg/mol. The volume fraction of the poly(α-methylstyrene) block is 0.20, and thus the expected morphology in the ordered state is hexagonally packed cylinders of poly(α-methylstyrene) in a polyisoprene matrix. The polydispersity of the MSI sample, measured by gel permeation chromatography, was 1.03, and the molar % of 3,4-isoprene units, measured by NMR, was 72%. The refractive indices of poly(α-methylstyrene) and polyisoprene are 1.59 and 1.52, respectively (room temperature, wavelength = 589 nm).[33]

The order−disorder transition of the MSI sample was determined by small-angle X-ray scattering and optical birefringence measurements to be 190 ± 5 °C. The glass transition of poly(α-methylstyrene) was determined by differential scanning calorimetry (10 °C/min scan) to be 150 °C. Films of the MSI sample were deposited on 2.54 cm diameter fused silica disks (for GWDLS) and on silicon substrates (for AFM) by spin-coating 15 wt % solutions of the polymer in toluene at 3000 rpm. Making samples on two different substrates was necessary because the silica substrates needed for the GWDLS experiments were larger than the maximum sample size that could be accommodated by our AFM. Substrates were cleaned with a single wash of toluene prior to spin-coating, as described by Harrison et al.[34] The resulting films were about 1 μm thick. Pairs of identical films deposited on fused silica and silicon substrates were processed in parallel. After spin-coating, the films were dried for 12 h in a vacuum oven at about 150 °C to drive off remaining solvent. These films are referred to as unannealed films. A fraction of these films were annealed, one pair at a time in a home-built, nitrogen-filled oven. Care was taken to place the fused silica and silicon pair as close to each other as possible in the oven to ensure that the thermal histories of each pair were identical. The films were initially heated rapidly to 181 °C. The sample temperature was decreased by 1.8 °C every 5 min until the sample temperature reached 163 °C. The heater was then turned off, and the samples were removed from the oven after they had cooled to room temperature. Independent measurements of the temperature gradients in the oven were made by placing thermocouples at various places in the oven. The maximum temperature difference between the fused silica and silicon pair is estimated to be 2 °C. All subsequent characterization was performed at room temperature.

A schematic of the GWDLS apparatus is shown in Figure 2a. A helium−neon laser, producing a plane-polarized beam of light with wavelength λ = 633 nm, serves as the source. The beam is directed through a variable neutral density filter and a set of beam steering mirrors into a beam splitter. A small portion of the incident beam is split here for monitoring

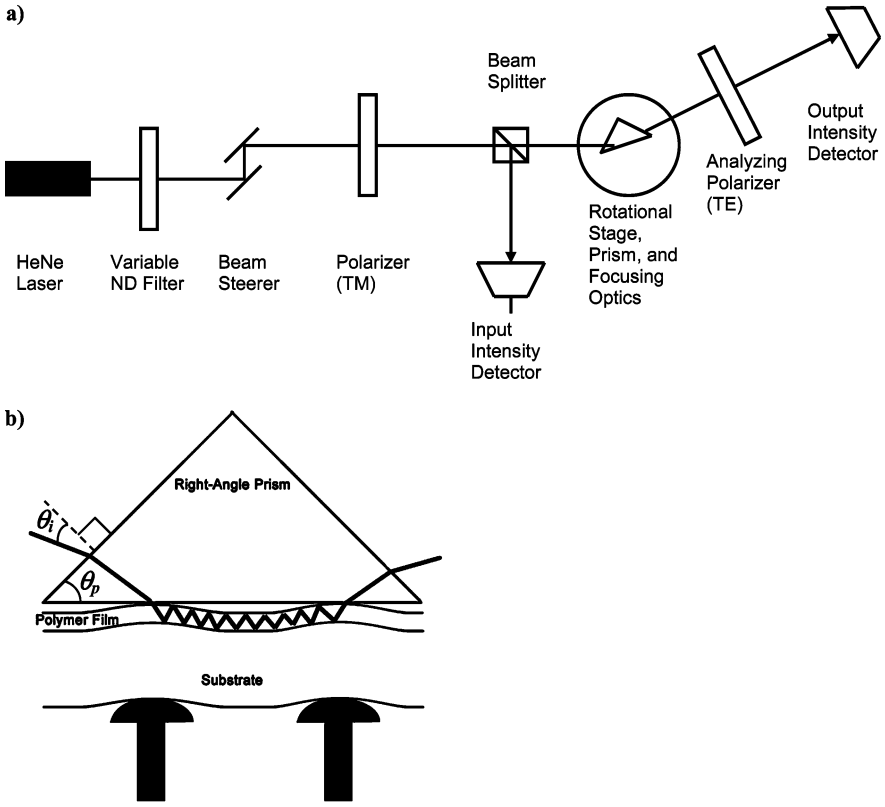

Figure 2. (a) Diagram of GWDLS apparatus. (b) Schematic of prism coupler.

purposes, while most of the beam, which is horizontally polarized, is directed toward the sample. The beam is coupled into the MSI film using a right angle prism coupler. The coupling between the block copolymer film and the prism is created by the action of two cap nuts pressing against the back of the silica substrate, as shown in Figure 2b. The cap nuts are screwed into 11 mm diameter pistons that are pressure actuated by air cylinders. The film/prism interface appears reflective when the piston pressure is low due to the presence of an air gap between the film and prism. With increasing pressure on the piston, this gap reduces in thickness due to deformation of the substrate and film, and at a particular pressure, a nonreflective coupling spot can be seen at the film/prism interface. These coupling spots are several millimeters in diameter, comparable to the diameter of the incident laser beam, and serve as points where the laser light is coupled into and out of the waveguide.[35] To couple laser light efficiently into the film, the angle of the input beam must correspond with one of the waveguide modes. To enable realization of this condition, the prism/film assembly is mounted on a horizontal rotary stage, with the prism−film interface oriented in a vertical plane. The waveguiding angles are readily identified by a marked decrease in the reflected light at the input coupling point and the appearance of output bands. Measurement of the angle of incidence of two waveguided modes enables determination of the thickness and refractive index of our films.[36,37] For completeness, we have included the formulas that enable this determination in the Preliminary Theoretical Considerations section below.

We define the direction of propagation of laser light within the film to be the z-axis. The y-axis is perpendicular to the z-axis and parallel to the film plane. The x-axis is perpendicular to the film plane. In the $y-z$ plane, the plane of the film, light can be scattered into all angles. In the $x-z$ plane, however, scattering is only allowed into certain discrete angles corresponding to the guided modes of the optical waveguide.[36,37] Light scattered within these modes appears as vertical lines on a screen placed behind the output coupling point. A cylindrical lens is used to focus a chosen line onto a photodetector to record the output signal, as shown in Figure 2a. A 2 mm wide vertical slit is fixed as a mask in front of the photodiode to reduce stray light reaching the detector. A movable analyzing polarizer is placed between the sample and the detector to block out the guided TM modes when the intensity of a depolarized TE mode is measured. The detector system (photodiode, lens, and analyzer) is mounted on an arm that is connected to the rotary table. This enables coarse prealignment of the detector. The photodiode is mounted on a rail to allow for easy translation in the direction perpendicular to the rail. This enables final alignment of the detector system.

We chose the MSI copolymer for our study for two reasons. First, the birefringence signal obtained from ordered, bulk MSI samples was significantly larger than those obtained from other block copolymers [e.g., poly(styrene-*block*-isoprene) copolymers]. Second, the methodology that we have used to couple the laser beam into the sample requires samples that do not deform significantly under the applied load of the two pressure actuated pistons. MSI copolymers are significantly stiffer than poly(styrene-*block*-isoprene) copolymers due to the high glass transition temperature of the poly(α-methylstyrene) block. These properties made MSI copolymers a convenient system for our initial studies with the GWDLS apparatus.

A Digital Instruments Multimode AFM and NanoScope IIIa controller were used to image film surfaces of the MSI films deposited on Si substrates. Tapping mode AFM was used to produce contrast between the soft isoprene and the harder α-methylstyrene phases. Nanosensors NCL-50 Pointprobe tips were autotuned in Digital Instruments' NanoScope Control 5.12r5, giving a drive frequency around 147 kHz and drive amplitudes below 100 mV. Qualitatively identical results were obtained from phase and height images. We chose to present exclusively phase data in this publication.

Preliminary Theoretical Considerations

The silica substrate−film interface is located at $x = 0$, and the film−cover interface is located at $x = L$. In our case, the cover is air. Our previous analysis of depolarized light scattering from ordered block copolymer samples in free space serves as a convenient

starting point for the analysis of the GWDLS signal.[25] In that work it was shown that the field scattered from a collection of randomly oriented grains is given by

$$\mathbf{E}_{\text{scattered}}(\mathbf{r}) \underset{\text{limit } r \gg r'}{=} -\epsilon_0^{-1} k^2 \int_V \mathrm{d}\mathbf{r}'\, \mathbf{G}(\mathbf{r}-\mathbf{r}') \sum_j \delta\epsilon_j f_j(\mathbf{r}')\, \mathbf{E}(\mathbf{r}') \quad (1)$$

where V is the illuminated sample volume, the summation index, j, labels the randomly oriented grains, $\delta\epsilon_j$ is the anisotropic part of the permittivity of the jth grain, $f_j(\mathbf{r}')$ is the shape factor for the jth grain (equal to 1 if $\mathbf{r}'$ is in the jth grain and 0 otherwise), $\mathbf{E}(\mathbf{r}')$ is the input field within the sample, and $\mathbf{G}(\mathbf{r}-\mathbf{r}')$ is the Green's function dyadic appropriate for the electromagnetic structure (waveguide) where the scattering takes place. In the case of depolarized light scattering in free space, $\mathbf{E}(\mathbf{r}')$ is a simple vector field oriented in the direction of the incident polarization. In the case of GWDLS, $\mathbf{E}(\mathbf{r}')$ is obtained by solving Maxwell's equations for the waveguide of interest. This solution is shown schematically in Figure 1, where the grazing angle inside the film is θ_g, corresponding to an angle of incidence θ_i into the prism, as shown in Figure 2b. For simplicity, we assume that our sample is of infinite extent in the y- and z-directions. The incident beam can, in principle, be either TE (y-polarized electric field) or TM (y-polarized magnetic field). In both cases, the electric and magnetic field amplitudes are of the form $u(x)\exp(i\beta z)$, which represents waves moving in the z-direction with a phase velocity ω/β, where ω is the angular frequency of the light. $u(x)$ satisfies

$$\frac{\mathrm{d}^2 u}{\mathrm{d}x^2} - (\beta^2 - n^2(x)k^2)u = 0 \quad (2)$$

where $n(x)$ is a piecewise continuous function describing the variation of refractive index in the x-direction, including the substrate ($x < 0$), film ($0 \le x \le L$), and air ($x > L$). Outside the film, the fields decay exponentially with respect to x, taking the forms $\exp(-\alpha_c x)$ and $\exp(\alpha_s x)$ in the cover and substrate, respectively. Within the film, u takes the form $\exp(i\kappa x) + \Gamma \exp(-i\kappa x)$. When combined with the $\exp(i\beta z)$, the field inside the film is seen to consist of two waves that make an angle $\tan^{-1}(\kappa/\beta)$ with the z-axis. The guided modes of interest here are obtained when these waves undergo constructive interference. A convenient method for obtaining the guided modes was proposed by Kogelnik and Ramaswamy[38] and Haus,[39] which requires the simultaneous solution of the following four equations

$$\tan(\kappa L) = \frac{\alpha_c/\kappa + (n_c/n_s)^{2\rho}\alpha_s/\kappa}{(n_c/n_f)^{2\rho} - (n_f/n_s)^{2\rho}(\alpha_s\alpha_c/\kappa)}$$

$$\beta^2 - \alpha_s^{\,2} = n_s^{\,2}k^2, \quad \beta^2 - \alpha_c^{\,2} = n_c^{\,2}k^2, \quad \beta^2 + \kappa^2 = n_f^{\,2}k^2 \quad (3)$$

where $k = \omega/c$ (c is the speed of light in vacuum), $\rho = \{0,1\}$ for {TE,TM} modes, and n_s, n_c, and n_f are the known refractive indices of the substrate, cover, and film, respectively. Equations 3 can be solved for β, α_s, α_c, and κ, which then can be used to find θ_g and θ_i (see Figures 1 and 2 for definitions), given by

$$\theta_g = \tan^{-1}(\kappa/\beta) \quad (4)$$

and

$$\theta_i = \theta_p - \pi/4 + \sin^{-1}(n_p \sin(-\theta_p + \sin^{-1}(n_f \cos\theta_g/n_p))) \quad (5)$$

where θ_p is the prism angle and n_p is the refractive index of the prism. In our case, $\theta_p = 45°$ and $n_p = 1.723$.

Having obtained $\mathbf{E}(\mathbf{r})$, one can compute $\mathbf{E}_{\text{scattered}}(\mathbf{r})$ using eq 1 for a given collection of grains, if the Green's function $\mathbf{G}(\mathbf{r}-\mathbf{r}')$ is known. In previous papers, we have obtained $\mathbf{G}(\mathbf{r}-\mathbf{r}')$ for scattering in free space.[25] A quantitative analysis of the waveguide structure would require the Green's function dyadic for this geometry. Expressions have been presented in terms of expansions in vector eigenfunctions in the radio wave context.[40,41] We plan to exploit this work in future calculations of the optical field properties, but for our present purposes we will deal with general aspects of the expected behavior. From this point onward, we assume that the incident polarization is TM, as was the case with the experiment. The waveguide structure affects scattering into waves in a manner that depends on the x- and z-components of their propagation vectors, but not on the y-component. It is thus neither appropriate to assume that the scattering occurs in free space nor that it occurs only in the waveguided modes. We can, however, make some general statements regarding the scattered field, based on the form of eq 1.

Equation 1 gives a general expression for the field that involves a sum of contributions from the N grains making up the sample. Each term in the sum will be proportional to the volume of the grain times an angular distribution factor that depends on the shape of the grain, the direction of its optic axis, and the Green's function of the waveguide. The scattered intensity is obtained by taking the absolute square of the sum and averaging over the grain orientations. Since there are N grains, there will be N^2 terms in the expression for the intensity, N of them from the diagonal elements corresponding to incoherent scattering and $N(N-1)$ terms arising from the interference of pairs of grains corresponding to coherent scattering. In the case of bulk scattering the coherent term leads to a large peak in the incident direction along with randomly located "speckles". The incoherent term leads to a scattering profile that is centered along the incident beam direction with an angular distribution that characterizes the shape of the grains. It has the form $Nv^2 f_{\text{bulk}}(\theta,\phi)$, where v is the average volume of the grains and the function $f_{\text{bulk}}(\theta,\phi)$ represents the angular dependence of the incoherent term. Here θ and ϕ are spherical polar angles of a spherical coordinate system centered at the intersection of the incident and scattered beams. When integrated over polar angles $\{\theta,\phi\}$, one gets the total scattered incoherent power which is proportional to Nvl, where l is the average grain length in the propagation direction. More detailed discussions of scattering from a collection of grains, including explicit expressions for $f_{\text{bulk}}(\theta,\phi)$, are given in previous work.[22-25]

In the case of scattering into waveguide modes, the propagation vectors have oppositely directed small x components and a common z component. Each grain thus has two induced dipole components, each phased to radiate into one of the two propagating directions of the TM mode. The optical anisotropy of the grain causes

depolarized light scattering in a range of directions about the two propagating vectors. For typical block copolymer films, the angle between the lowest TM and TE modes is about 0.01 rad (eqs 3). Since these beams are well resolved, the incident TM beam does not scatter coherently into the TE modes, except for the speckles. Nevertheless, that angle is small enough that there can be strong incoherent scattering into TE modes. Thus, the depolarized power per unit solid angle scattered into the TE modes should have the dependence $Nv^2 \cdot f_{\text{waveguide}}(\theta,\phi)$, where $f_{\text{waveguide}}(\theta,\phi)$ is the angular dependence of the incoherent scattering due to the grain structure and the Green's function of the waveguide. By dimensional analysis it follows that the dependence on grain shape is through ratios of the grain dimensions to the wavelength of light. The function $f_{\text{waveguide}}(\theta,\phi)$ is expected to behave like a product of $f_{\text{bulk}}(\theta,\phi)$ and the waveguide response function, which contains strong resonances at the angles corresponding to the waveguide modes. If we consider just the total scattered power into the lowest TE mode, then the angular spread in the x-direction would be fixed by the waveguide response function and in the y-direction would be proportional to (λ/w), where w is the average grain length in the y-direction. Then the total scattered power into the mode would be proportional to $\Phi Nv^2/w$, where Φ is the fraction of all the scattered power into the lowest TE mode. It is thus clear that the GWDLS signal will be proportional to both the number of grains per unit volume and grain size. In this respect, GWDLS data for a film are analogous to DPLS data from bulk samples.

Thus, GWDLS can, in principle, be used to determine the order−disorder transitions and study the kinetics of grain growth in block copolymer thin films. Imperfections in the sample, such as dust particles and irregularities at the interfaces at $x = 0$ and $x = L$, may, in some cases, lead to excitation of the TE mode. The GWDLS experiment will be useful only if the TE contribution due to the grains is significantly larger than that due to imperfections.

Film Characterization by GWDLS and AFM

A GWDLS experiment begins by placing the polymer-coated substrate on the prism coupler and applying the minimum pressure on the pistons to obtain the coupling spots. After this is done, the piston pressure is recorded and held constant until the experiment is completed. Typical pressures are 200−450 kPa. The rotary stage is rotated to determine the number of available waveguide modes and their respective coupling angles. Our $\sim$1 μm thick MSI films supported two guided TM modes, with angles of incidence in the range $\theta_{i,0} = 30.2 \pm 0.5°$ and $\theta_{i,1} = 23.4 \pm 0.6°$. Substituting $n_s = 1.46$, $n_c = 1$ into eqs 3 gives $n_f = 1.541 \pm 0.003$ and $L = 1.03 \pm 0.06$ μm. Typical output beams obtained when coupling into the zeroth-order TM mode are shown in Figure 3. Here we have replaced the detector by a white piece of paper. The two streaks of light correspond to the $m = 0$ and $m = 1$ TM modes that are coupled out of the prism. The bright spot in the center of the $m = 0$ streak is the original TM mode that was excited by the incident beam. The observation of the streak around the spot is due to polarized light scattering from imperfections in the film and substrate. The $m = 1$ mode is also excited due to scattering from imperfections in the film and substrate. Tien has shown that surface imperfections have a greater contribution to scattering than bulk imperfections.[36]

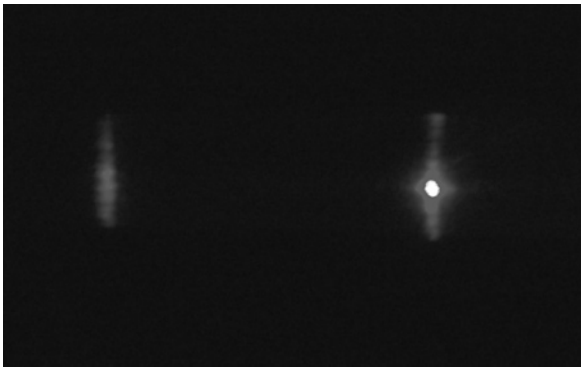

Figure 3. Output bands from a typical ordered MSI film, as seen on a piece of white paper placed in the detector's position, shown with cylindrical focusing lens in place. The brighter line on the right is the $m = 0$ TM mode, and the weaker line on the left is the $m = 1$ TM mode.

With the rotary stage in the $\theta_{i,0}$ position, and the analyzer removed from the optical path, fine rotation control of the rotary stage is used to maximize the detector signal. The variable neutral density filter is rotated to prevent saturation of the detector. Final maximization of the signal is accomplished by translating the detector. The photodiode signal thus recorded is S_{tot}, which represents the sum of the incident TM_0 and the scattered TE_0 beams. The input monitor photodiode signal, S_{mon}, is also recorded at this time. The normalized total transmitted intensity I_0 is given by

$$I_0 = A(S_{\text{tot}} - b_{\text{d}})/(S_{\text{mon}} - b_{\text{m}}) \tag{6}$$

where A is the transmission coefficient of the polarizer (determined to be 0.388 ± 0.003, and necessary because the polarizer is not in place for this measurement, but is in place while measuring TE mode intensity), and b_{d} and b_{m} are the background signals of the detector and monitor, respectively, obtained with the laser turned off. The analyzer is then put in place, and the detector signal is measured after fine-tuning the position of the detector. The TE_0 mode is obtained at a slightly more grazing angle with respect to the z-axis than the TM_0 mode, and this fine adjustment of the detector position is required to maximize the measured signal. During this measurement, the variable neutral density filter is set for maximum transmission. The TE modes are much fainter than the TM modes and are thus not visible in Figure 3. The measured signal in this configuration, which we call S_{TE}, gives the normalized GWDLS intensity I

$$I = (S_{\text{TE}} - b_{\text{d}})/(S_{\text{mon}} - b_{\text{m}}) \tag{7}$$

where S_{mon} has to be recorded again due to changes in the neutral density filter setting.

Six independent measurements of the ratio I/I_0 were made of each film. The film was rotated by approximately 60° between measurements to obtain independent paths for the propagating light beam. The fraction of the laser beam that coupled into and back out of a given film routinely varied by over an order of magnitude, due mainly to variability in the size and shape of the coupling points.

We present GWDLS and AFM data obtained from seven pairs of films, four unannealed films (U1, U2, U3, and U4) and three annealed films (A1, A2, and A3). The results of these experiments are summarized in Table

Table 1. GWDLS Scattering and AFM Data Summary for Annealed Film Pairs A1−A3 and Unannealed Film Pairs U1−U4

sample ID and description	I/I_0	AFM results
A1	$(1.6 \pm 0.3) \times 10^{-2}$	long-range order observed
A2	$(1.9 \pm 0.5) \times 10^{-2}$	long-range order observed
A3	$(1.7 \pm 0.5) \times 10^{-2}$	long-range order observed
set of A1−A3	$(1.7 \pm 0.2) \times 10^{-2}$	
U1	$(6 \pm 1) \times 10^{-3}$	no long-range order observed
U2	$(5 \pm 2) \times 10^{-3}$	some microphase separation apparent, but no long-range order observed
U3	$(2 \pm 1) \times 10^{-3}$	some microphase separation apparent, but no long-range order observed
U4	$(5 \pm 1) \times 10^{-3}$	no long-range order observed
set of U1−U4	$(5 \pm 2) \times 10^{-3}$	

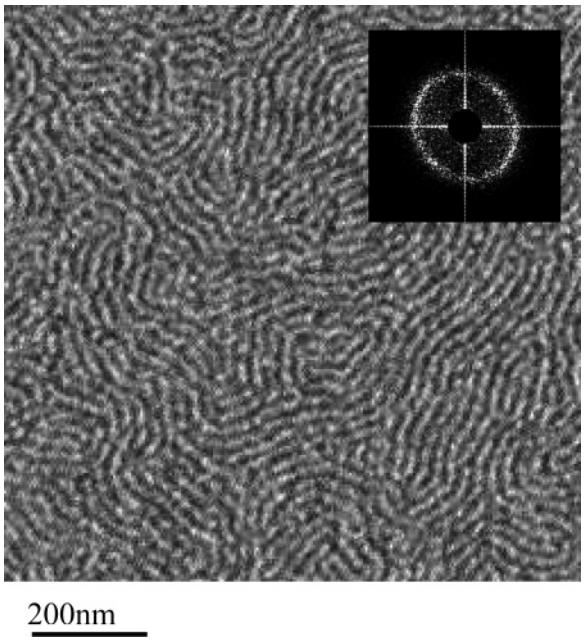

Figure 4. AFM phase image from annealed sample A1. The inset shows a Fourier transform of these data with the bright central spot masked.

1. The I/I_0 values for the annealed samples averaged $(1.7 \pm 0.2) \times 10^{-2}$. In the unannealed samples, the I/I_0 average was $(5 \pm 2) \times 10^{-3}$. It is clear that the annealed samples show a significantly higher value of I/I_0 than the unannealed samples.

Several AFM images were obtained from each of the films listed in Table 1. All of the images obtained from the annealed films showed the presence of a cylindrical structure with significant long-range order. Typical results are displayed in Figure 4, where we show one of the AFM phase images obtained from sample A1. In contrast, the AFM micrographs obtained from the unannealed samples did not show any sign of long-range order. Most of the images were completely featureless. Figure 5a, where we show a phase scan from sample U4, is an example of such images. In a few cases, we were able to detect signs of weak microphase separation in the unannealed films. Figure 5b, where we show data from sample U2, shows the AFM scan with the most clearly discernible features out of all of the unannealed samples studied. The two images in Figure 5 thus encompass the range of AFM data obtained from our unannealed films. The Fourier transforms of each of the AFM images are shown in the insets in Figures 4 and 5. The presence of a well-developed ring in the Fourier transform of A1 (Figure 4) indicates the presence of a periodic structure with long-range order, while the absence of rings in the Fourier transforms of U2 and U4 (Figure 5) indicates the absence of a periodic structure. It is clear from Table 1 and Figures 4 and 5 that samples with a well-developed grain structure, as determined by AFM, give consistently larger GWDLS signals than those with a poorly developed grain structure.

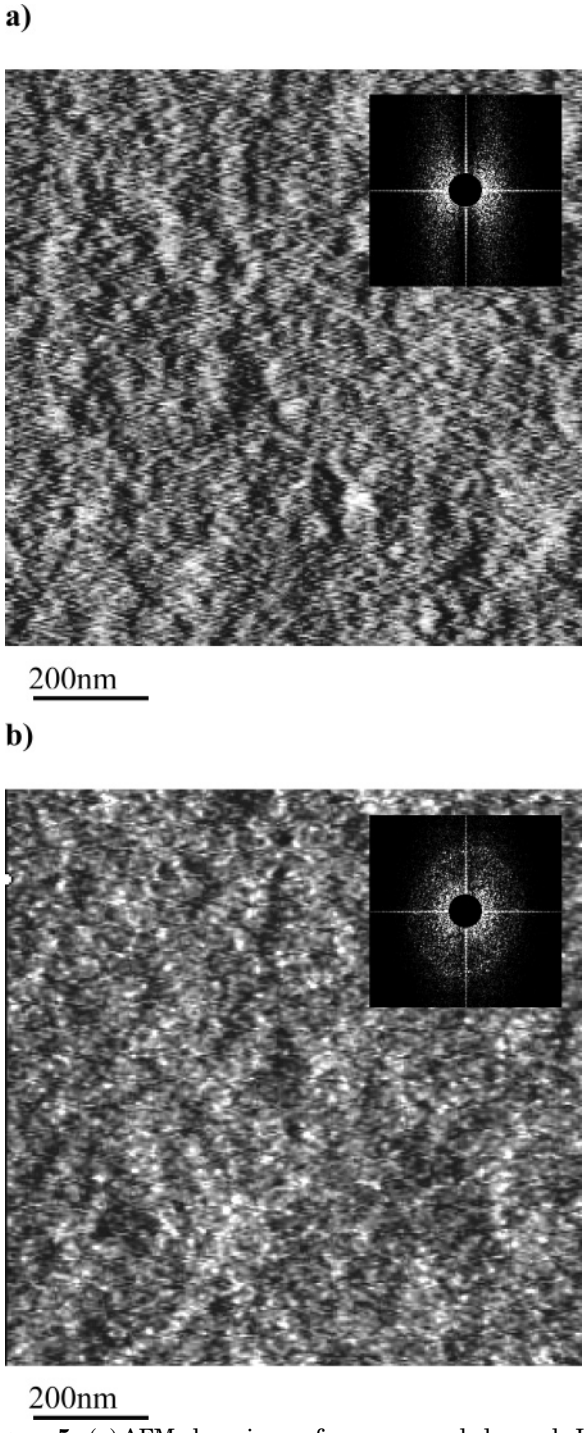

Figure 5. (a) AFM phase image from unannealed sample U4. (b) AFM phase image from unannealed sample U2. The insets show Fourier transforms of these data with the bright central spots masked.

Conclusion

The main purpose of this paper is to describe a new technique for studying the state of order in block copolymer thin films. We call this technique guided wave depolarized light scattering. A polarized beam of light interacts with ordered grains in the thin film, leading to the creation of depolarized light. We show that the magnitude of the depolarized light scattering signal is consistent with the grain structure of the film, as determined by AFM.

The present work is limited in many ways. The theory section of this paper is limited to qualitative discussion of the relationship between the GWDLS signal and grain structure. Our characterization of thin films in position space is restricted to the top surface of the films. In the future, we will use other techniques such as cross-sectional TEM and reactive ion etching to examine the grain structure inside our films. In the current asymmetric geometry with silica as the substrate for the waveguide and air as the cover, we can only study block copolymer films that are thicker than 260 nm (i.e., for $n_s = 1.46$, $n_f = 1.56$, and $n_c = 1.0$, eqs 3 have no solution for films with $L < 260$ nm).[42] Our current approach to coupling light into the film requires hard thin films that are not significantly deformed by the force applied by the input and output coupling pistons. The present apparatus thus cannot be used to study samples near the order−disorder transition temperature because samples become soft and liquidlike in the disordered state. Similar problems will arise if the present apparatus is used to study the kinetics of the disorder-to-order transition. There are, however, modifications that can be used to address these limitations. One could, for example, reduce the deformation of the sample by using spacers (glass beads that are not in the optical path) and a silica cover and use optical gratings to couple light into and out of the thin film.[43,44] The addition of the silica cover will make the waveguide symmetric, wherein guided modes are obtained for any sample thickness (i.e., if $n_s = n_c = 1.46$ and $n_f = 1.56$, eqs 3 have at least one solution for all values L).[45] Despite the limitations, we believe that the present work represents an important first step in using polarized light to study the state of order in block copolymer thin films.

Acknowledgment. Financial support was provided by the National Science Foundation (DMR-0213508 and DECS 0103297). We thank Dr. John H. Jackson, president of Metricon Corp., for his advice on methods for coupling light into thin polymer films and Hany B. Eitouni for his help in fabricating the GWDLS apparatus.

References and Notes

(1) Park, M.; Harrison, C.; Chaikin, P. M.; Register, R. A.; Adamson, D. H. *Science* **1997**, *276*, 1401.
(2) Thurn-Albrecht, T.; Schotter, J.; Kastle, C. A.; Emley, N.; Shibauchi, T.; Krusin-Elbaum, L.; Guarini, K.; Black, C. T.; Tuominen, M. T.; Russell, T. P. *Science* **2000**, *290*, 2126.
(3) Segalman, R. A.; Yokoyama, H.; Kramer, E. J. *Adv. Mater.* **2001**, *13*, 1152.
(4) Urbas, A.; Fink, Y.; Thomas, E. L. *Macromolecules* **1999**, *32*, 4748.
(5) Fink, Y.; Urbas, A. M.; Bawendi, M. G.; Joannopoulos, J. D.; Thomas, E. L. *J. Lightwave Technol.* **1999**, *17*, 1963.
(6) Russell, T. P.; Karim, A.; Mansour, A.; Felcher, G P. *Macromolecules* **1998**, *21*, 1890.
(7) Foster, M.; Stamm, M.; Reiter, G.; Huttenbach, S. *Vacuum* **1990**, *41*, 1441.
(8) Reiter, G. *Macromolecules* **1994**, *27*, 3046.
(9) Briggs, D.; Wootton, A. B. *Surf. Interface Anal.* **1982**, *4*, 109.
(10) Briggs, D.; Hearn, M. J. *Spectrochim. Acta B* **1985**, *40*, 707.
(11) Binning, G.; Quate, C. F.; Gerber, C. *Phys. Rev. Lett.* **1986**, *56*, 930.
(12) Knoll, A.; Magerle, R.; Krausch, G. *Macromolecules* **2001**, *34*, 4159.
(13) Vezie, D. L.; Thomas, E. L.; Adams, W. W. *Polymer* **1995**, *36*, 1761.
(14) Kunz, M.; Shull, K. *Polymer* **1993**, *34*, 2427.
(15) Muller-Buschbaum, P.; Vanhoorne, P.; Scheumann, V.; Stamm, M. *Europhys. Lett.* **1997**, *40*, 655.
(16) Muller-Buschbaum, P.; Casagrande, M.; Gutmann, J.; Kuhlmann, T.; Stamm, M.; von Krosigk, G.; Lode, U.; Cunis, S.; Gehrke, R. *Europhys. Lett.* **1998**, *42*, 517.
(17) Muller-Buschbaum, P. *Anal. Bioanal. Chem.* **2003**, *376*, 3.
(18) Harrison, C.; Chaikin, P. M.; Huse, D. A.; Register, R. A.; Adamson, D. H.; Daniel, A.; Huang, E.; Mansky, P.; Russell, T. P.; Hawker, C. J.; Egolf, D. A.; Melnikov, I. V.; Bodenschatz, E. *Macromolecules* **2000**, *33*, 857.
(19) Lodge, T. P.; Fredrickson, G. H. *Macromolecules* **1992**, *25*, 5643.
(20) Balsara, N. P.; Perahia, D.; Safinya, C. R.; Tirrell, M.; Lodge, T. P. *Macromolecules* **1992**, *25*, 3896.
(21) Balsara, N. P.; Garetz, B. A.; Dai, H. J. *Macromolecules* **1992**, *25*, 6072.
(22) Garetz, B. A.; Newstein, M. C.; Dai, H. J.; Jonnalagadda, S. V.; Balsara, N. P. *Macromolecules* **1993**, *26*, 3151.
(23) Dai, H. J.; Balsara, N. P.; Garetz, B. A.; Newstein, M. C. *Phys. Rev. Lett.* **1996**, *77*, 3677.
(24) Newstein, M. C.; Garetz, B. A.; Balsara, N. P.; Chang, M. Y.; Dai, H. J. *Macromolecules* **1998**, *31*, 64.
(25) Wang, H.; Newstein, M. C.; Chang, M. Y.; Balsara, N. P.; Garetz, B. A. *Macromolecules* **2000**, *33*, 3719.
(26) Kim, W. G.; Chang, M. Y.; Garetz, B. A.; Newstein, M. C.; Balsara, N. P.; Lee, J. H.; Hahn, H.; Patel, S. S. *J. Chem. Phys.* **2001**, *114*, 10196.
(27) Kim, W. G.; Garetz, B. A.; Newstein, M. C.; Balsara, N. P. *J. Polym. Sci., Polym. Phys.* **2001**, *39*, 2231.
(28) Hanley, K. J.; Lodge, T. P.; Huang, C. I. *Macromolecules* **2000**, *33*, 5918.
(29) Bailey, T. S.; Hardy, C. M.; Epps, T. H.; Bates, F. S. *Macromolecules* **2002**, *35*, 7007.
(30) Migler, K. B.; Han, C. C. *Macromolecules* **1998**, *31*, 360.
(31) RamachandraRao, V. S.; Watkins, J. J. *Macromolecules* **2000**, *33*, 5143.
(32) Burghardt, W. R.; Hongladarom, K. *Macromolecules* **1994**, *27*, 2327.
(33) Bicerano, J. *Prediction of Polymer Properties*; Marcel Dekker: New York, 1993.
(34) Harrison, C.; Park, M.; Chaikin, P.; Register, R. A.; Adamson, D. H.; Yao, N. *Macromolecules* **1998**, *31*, 2185.
(35) Our optical coupling technique is based on that used in the Metricon Model 2010 prism coupling instrument.
(36) Tien, P. K. *Appl. Opt.* **1971**, *10*, 2395.
(37) Ulrich, R.; Torge, R. *Appl. Opt.* **1973**, *12*, 2901.
(38) Kogelnik, H.; Ramaswamy, V. *Appl. Opt.* **1974**, *13*, 1857.
(39) Haus, H. A. *Waves and Fields in Optoelectronics*; Prentice Hall: Englewood Cliffs, NJ, 1984.
(40) Cavalcante, G. P. S.; Giarola, A. J. *IEEE T. Antenn. Propag.* **1983**, *31*, 141.
(41) Li, L. W.; Koh, J. H.; Yeo, T. S.; Leong, M. S.; Kooi, P. S. *IEEE T. Antenn. Propag.* **2004**, *52*, 466.
(42) Yariv, A.; Yeh, P. *Optical Waves in Crystals: Propagation and Control of Laser Radiation*; John Wiley & Sons: New York, 1984.
(43) Tamir, T.; Peng, S. T. *Appl. Phys.* **1977**, *14*, 235.
(44) Moshrezadeh, R.; Mai, X.; Seaton, C. T.; Stegeman, G. I. *Appl. Opt.* **1987**, *26*, 2501.
(45) Although there is no theoretical lower limit to the film thickness for propagating modes in the symmetric waveguide, there is certainly a practical limit due to the fact that the propagating mode has evanescent tails that extend into the substrate and cover, so that as the film gets thinner and thinner, most of the propagating wave is sampling the substrate and cover rather than the film, and the total scattering signal becomes due primarily to scattering in the substrate and cover rather than the film. The thinner the film, the greater the contribution to the scattering from the substrate and cover, and thus the lower the signal-to-noise ratio.

MA047859B